

# Periodical Plasma Structures Controlled by Oblique Magnetic Field

I. V. Schweigert<sup>1,2</sup> and M. Keidar<sup>1</sup>

<sup>1</sup>*George Washington University, Washington D.C. 20052, USA*

<sup>2</sup>*Khristianovich Institute of Theoretical and Applied Mechanics, Novosibirsk 630090, Russia*

(Dated: November 17, 2018)

The propulsion type plasma in oblique external magnetic field is studied in 2D3V PIC MCC simulations. A periodical structure with maxima of electron and ion densities appears with an increase of an obliqueness of magnetic field. These ridges of electron and ion densities are aligned with the magnetic field vector and shifted relative each other. As a result the two-dimensional double-layers structure forms in cylindrical plasma chamber. The ion and electron currents on the side wall are essential modulated by the oblique magnetic field.

PACS numbers: 52.40.Kh, 52.40.Hf, 52.65.Rr

## INTRODUCTION

Recently some methods to control the Hall effect thruster characteristics with applying the oblique magnetic field with respect to the channel walls is widely discussed (see, [1, 2] and references cited therein). Nevertheless with increasing the inclination of the magnetic field, discharge plasma properties can essentially change. For example, a several stationary, magnetized, two-dimensional weak double-layers were observed in a laboratory experiment for this type of plasma by Intrator, Menard, Hershkowitz [3]. The double-layer potential drops were found to be followed across any given potential profile. Borovsky, Joyce [4] showed in PIC simulations that weak magnetization results in the double-layer electric-field alignment of particles accelerated by these potential structures and that strong magnetization results in their magnetic-field alignment. A morphological invariance in two-dimensional double-layers with respect to the degree of magnetization observed in Ref. [4] implied that the potential structures scale with Debye lengths rather than with gyroradii.

A weak double-layer is a nonlinear electrostatic structure in plasmas, consisting of two sheets of positive and negative charges, with a characteristic electric potential jump, providing local electric field. Recently, most of the studies have addressed strong or ion acoustic double-layer in magnetized plasmas (see for example [5–9], while the mechanism of weak two dimensional double-layer formation is still not fully understood.

The motivation of our recent study is irregularities observed in Refs. [3, 10] in bounded low pressure discharge plasma induced by application of an oblique magnetic field. These irregularities seems similar to aurora-like periodical forms induced in ionosphere plasma with solar wind and interplanetary magnetic field (see [11] and references therein).

In this paper, in kinetic simulations we consider the direct current discharge plasma in the external oblique magnetic field at low gas pressure,  $P=10^{-4}$  Torr. Our purpose is to study the plasma structure modification

with changing the obliqueness and strength of magnetic field for the plasma parameters similar to the Hall thruster ones. We also consider the effect of obliqueness of magnetic field of the plasma-wall transition sheath in Hall thruster type plasma since the magnetic lens can be used to focus the ion flux.

## THEORETICAL MODEL AND CALCULATION DETAILS

In our simulations, the plasma is embedded in a cylindrical chamber with the radius of 4 cm and the height of 10 cm. The calculation domain is shown in Fig.1. The cathode with the radius of 3 cm is placed 0.3 cm

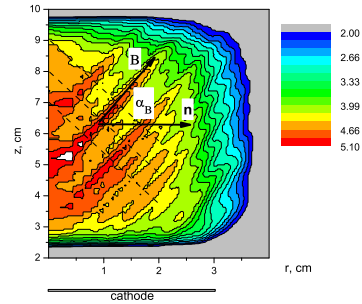


FIG. 1: Distribution of potential (V) for  $B=50$  G,  $\alpha_B = 65^\circ$  and  $T_e=5$  eV.  $B$  is the magnetic field vector,  $n$  is a normal to the side wall,  $\alpha_B$  is the angle between  $B$ -vector and  $n$ . Cathode is at  $z = 0.3$  cm.

apart from the chamber bottom. All walls of the chamber are grounded and the cathode is biased with  $-90$  V. The strength of external magnetic field  $B$  is assumed to be constant over the plasma volume. The magnetic field is axially symmetrical. To avoid the singularity at  $r=0$ , we took the magnetic field angle  $\alpha_B$  in the following form:  $\alpha_B=0$  at  $r<0.3$  cm,  $\alpha_B = \alpha_{B0}$  at  $r>0.6$  cm,  $\alpha_B$  is approximated by a spline-function at  $0.3 \text{ cm}<r<0.6$  cm. The  $\alpha_{B0}$  ranges from 0 to  $77^\circ$  in different variants.

To describe the plasma in electro-magnetic field at low gas pressure we solve Boltzmann equations (two dimensional in space and three dimensional in velocity space) for the distribution functions for electrons  $f_e(\vec{r}, \vec{v})$  and ions  $f_i(\vec{r}, \vec{v})$

$$\frac{\partial f_e}{\partial t} + \vec{v}_e \frac{\partial f_e}{\partial \vec{r}} - \frac{e(\vec{E} + \vec{v}_e \times \vec{B})}{m} \frac{\partial f_e}{\partial \vec{v}_e} = J_e, \quad n_e = \int f_e d\vec{v}_e, \quad (1)$$

$$\frac{\partial f_i}{\partial t} + \vec{v}_i \frac{\partial f_i}{\partial \vec{r}} + \frac{e(\vec{E} + \vec{v}_i \times \vec{B})}{M} \frac{\partial f_i}{\partial \vec{v}_i} = J_i, \quad n_i = \int f_i d\vec{v}_i, \quad (2)$$

where  $v_e, v_i, n_e, n_i, m, M$  are the electron and ion velocities, densities and masses, respectively.  $J_e, J_i$  are the collisional integrals for electrons and ions. No magnetic field due to currents in the plasma is taken into account. The Poisson equation describes the electrical potential and electrical field distributions

$$\Delta \phi = 4\pi e (n_e - n_i), \quad \vec{E} = -\frac{\partial \phi}{\partial \vec{r}}. \quad (3)$$

The system of equations (1)-(3) is solved with the 2D3V Particle-in-cell Monte Carlo collision method (PIC MCC) with PlasmaNOV code [12]. For electrons the elastic scattering, excitation and ionization were taken into account with the cross sections from Refs.[13, 14]. For ions the resonant charge exchange collisions with background argon gas are included. First, solving Eqs. (1)-(2), we calculate the electrical charge distribution, then the Poisson equation is solved to find a map of the electrical potential. The Poisson equation is solved on each electron time step. The steady-state solution is reached by iteration method.

The boundary conditions are the following:  $\phi = -90$  V at the cathode,  $\phi = 0$  at the wall of chamber and  $\delta\phi/\delta r = 0$  at  $r=0$ . Ions and electrons approaching the surface disappear from the calculation domain. The electron emission from the surface is not included in the model.

Additionally to the electron impact ionization the external ionization is included in the model. The external ionization is modeled as electron-ion pairs generation with the Maxwellian distributions over velocity with the mean electron temperature  $T_e$  and the ion temperature  $T_i = 0.05$  eV. The electron temperature  $T_e$  varies from 2.5 eV to 10 eV for different cases. The rate  $\nu_i$  of the electron-ion pair generation is chosen to achieve the plasma density of  $10^8 \text{cm}^{-3}$  in quasineutral part. For all cases the rate  $\nu_i$  is equal to  $2.5 \times 10^8 \text{s}^{-1} \text{cm}^{-3}$ .

In simulations, a strength of magnetic field  $B$  is ranged from 25 G to 100 G and the angle  $\alpha_B = 0 - 77^\circ$ . For these plasma parameters the electron Larmor radius  $r_L$  is comparable to the Debye length  $\lambda_D$ ,  $r_L \approx \lambda_D$ . The plasma frequency  $\omega_p$  is about of the electron gyrofrequency  $\Omega_e$ ,  $\omega_p \leq \Omega_e = 5 \times 10^8 \text{s}^{-1} - 5 \times 10^9 \text{s}^{-1}$ . In simulations, the electron time step  $\Delta t_e$  is  $(2-5) \times 10^{-12} \text{s}$ ,

so  $\Delta t_e \ll 1/\omega_p, 1/\Omega_e, \Delta r/v_e, \Delta z/v_e$ , where  $\Delta r, \Delta z$  are steps of calculation grid over axes  $r$  and  $z$ , and  $v_e$  is the maximum electron velocity.

The calculation grid is uniform over  $z$ -direction and nonuniform over radius condensing with increasing  $r$ . The total number of pseudo particles being chosen so that there is an average of approximately 100 positive and negative particles per Debye sphere. The electron/ion mass ratio is chosen to be a real one.

## EFFECT OF MAGNETIC FIELD ANGLE

In PIC MCC simulations, we found that a rearrangement of plasma begins with increasing obliqueness of B-field. For small  $\alpha_B = 10^\circ$  and  $27^\circ$  shown in Fig.2(a) and (b), the electron density is almost uniform in the central part of the chamber. In general, the plasma looks

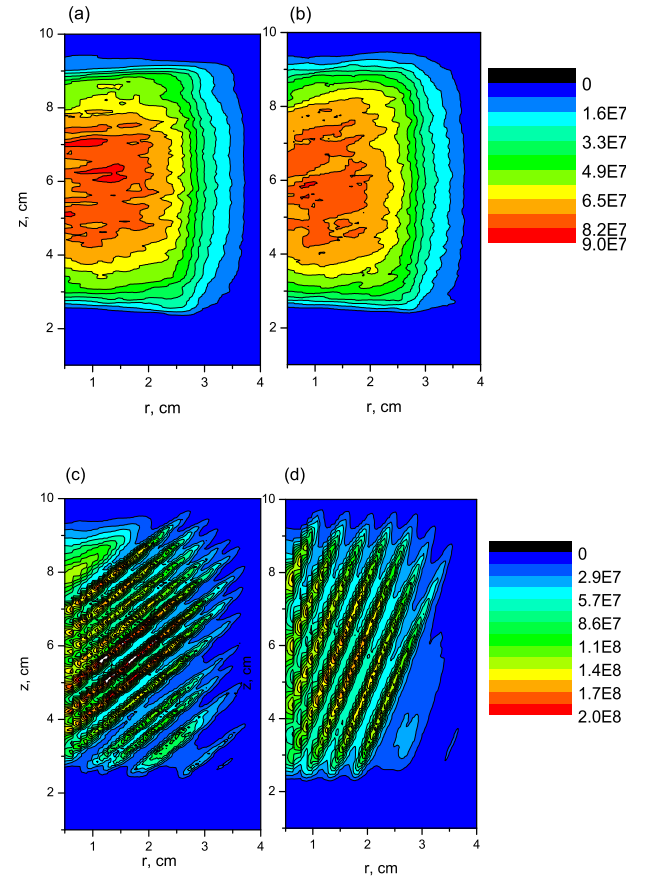


FIG. 2: Electron density distribution  $n_e, \text{cm}^{-3}$ , for  $\alpha_B = 10^\circ$ (a),  $27^\circ$ (b),  $55^\circ$ (c) and  $77^\circ$ (d),  $B=50$  G,  $T_e=2.5$  eV.

very similar to the case of  $\alpha_B=0$ . The developed sheath forms near the cathode with the potential drop of approximately 93 V. A weaker sheath screens plasma from walls of the chamber with the potential drop  $\delta\phi_w \approx 3$

V. The sheaths can be seen in Fig.2 as areas with the depleted electron density.

With increasing  $\alpha_B$  the periodical plasma structure becomes clearly visible (see Fig.2(c) and (d)). The structure occupies the quasineutral part of plasma in which the electrical field is small. Within the cathode sheath it does not appear even for large  $\alpha_B$ . More complex situation takes place in the wall sheath. As the potential drop over the wall is small ( $\delta\phi_w=3$  V - 8 V), the Lorentz and electrical forces are comparable there. Therefore the wall sheath becomes modulated by B-field with increasing  $\alpha_B$ .

In Fig.3(a) and (b), the electron  $j_e$  and ion  $j_i$  currents near the wall are shown for two values of  $\alpha_B$ . It is seen that both currents approaching the wall are affected by a variation of  $\alpha_B$ . The  $j_e$ -profile over  $z$  taken at  $r=3$  cm is almost uniform for  $\alpha_B=10^\circ$  and has peaks for  $\alpha_B=65^\circ$ . Each electron current peak is splitted with a scale of  $2r_L$ , where  $r_L$  is Larmor radius. The  $j_i$ -profile over  $z$  taken near the wall also exhibits peaks for larger  $\alpha_B$ . The  $j_i$  is about 20 time less than the  $j_e$ , but both clearly indicate the periodical plasma structure. An increase of the ion current and its peaked profile are typically observed in our simulations for larger  $\alpha_B$ . This effect can lead to an additional local erosion of wall material.

The insert in Fig.3, for  $\alpha_B=65^\circ$ , shows the potential distribution near the side wall. It is seen that the wall sheath is disturbed with the oblique magnetic field with large  $\alpha_B$ . The sheath potential exhibits the nonmonotonic distribution within the presheath which is getting smoother close to the wall.

The ion current profile within the cathode sheath is given in Fig.3(c) for two values of  $\alpha_B=10^\circ$  and  $65^\circ$ . The ion current increases by factor of 4 from  $z=3.5$  cm to  $z=1.5$  cm, both for small and large  $\alpha_B$ , as the electrical field increases within the sheath closer to the cathode. The some focusing effect of the oblique magnetic field on the ion flux can be seen for  $\alpha_B=65^\circ$ .

The current flow and ridges of electron and ion densities are aligned with  $B$ -vector not only in the area of quasineutral plasma, but also within the sheath over the wall. Only in the cathode sheath the ion current is directed normally to the surface.

### MULTIPLE LAYERS STRUCTURE

In Fig.4, the charge ( $n_e - n_i$ ) and potential distributions are shown for  $T_e=5$  eV and  $B=50$  G ( $r_L=0.105$  cm). The charge distribution has negative and positive ridges, both with an absolute value of  $0.27 \times 10^8 \text{cm}^{-3}$ . The sheets of large negative and positive charges appear in quasineutral plasma due to relative shift of  $n_e$  and  $n_i$ -ridges in the direction of increasing potential and across B-field. This structure is called as double-layers and characterized with the non-monotonic potential distribution shown in Fig.1. Cross sections of the potential distri-

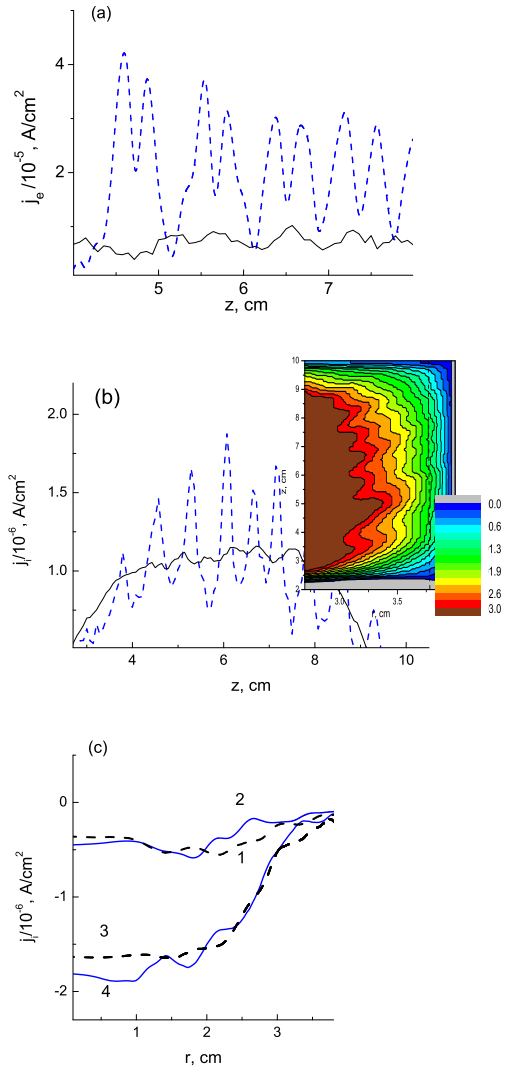


FIG. 3: (a) Electron current density distribution over  $z$  at  $r=3$  cm, (b) ion current density over  $z$  near side wall for  $\alpha_B=10^\circ$  (solid line) and  $\alpha_B=65^\circ$  (dashed line), insert shows the potential distribution (V) near the side wall  $\alpha_B=65^\circ$ , (c) ion current density in the cathode sheath at  $z=3.5$  cm (1),  $1.5$  cm (3) for  $\alpha_B=10^\circ$  and  $z=3.5$  cm (2),  $1.5$  cm (4) for  $\alpha_B=65^\circ$ .

bution across B-field is shown in Fig.4(b). These cross sections are taken along the dashed lines shown in Fig.1, which start at  $r=0$  and  $z=7$  cm,  $8$  cm,  $9$  cm. For this case the potential bumps across  $B$ -vector is about  $0.5$  V. Note that along  $B$ -vector the potential bumps are smaller ( $0.15$  V). The presence of magnetic field enhances the charge separation across  $B$ -vector.

For the close  $r_L=0.075$  cm, but for larger  $T_e=10$  eV and  $B=100$  G, the plasma parameters in Fig.5 look similar to the case shown in Fig.4. The electron density has maxima and minima  $1.3 \times 10^8 \text{cm}^{-3}$  and  $0.4 \times 10^8 \text{cm}^{-3}$ , respectively. The negative and positive charge densities are  $\mp 0.25 \times 10^8 \text{cm}^{-3}$ . The potential profiles shown in

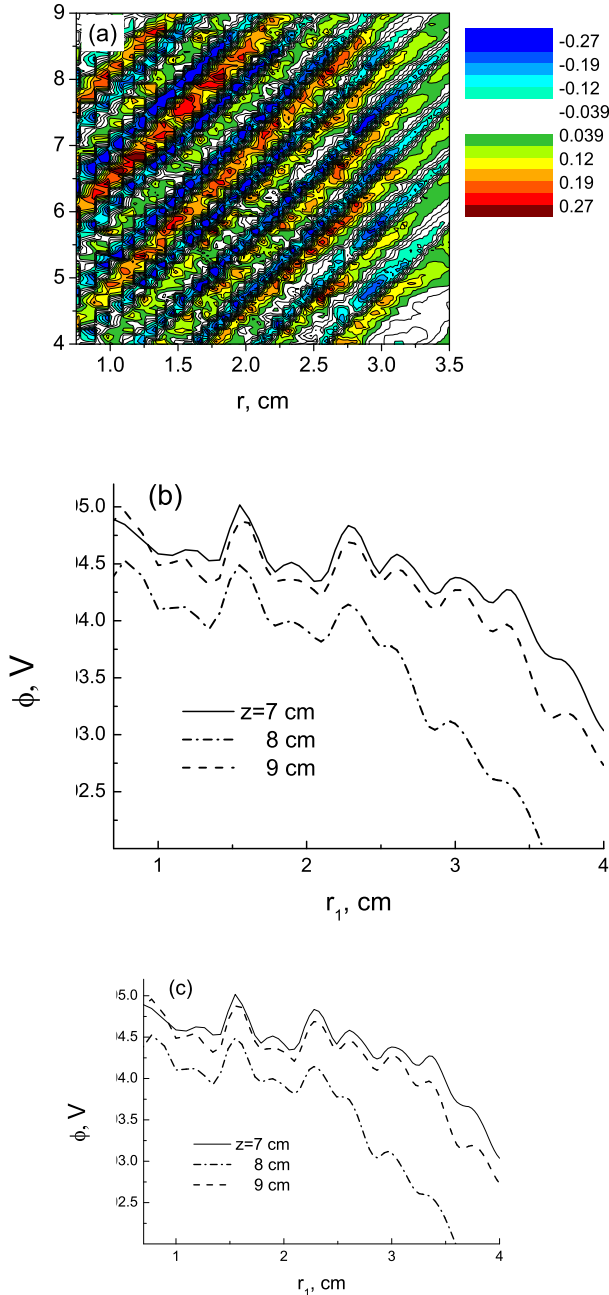


FIG. 4: Distributions of charge  $(n_e - n_i)/10^8 \text{ cm}^{-3}$  (a), and potential profile along axis  $r_p$ , which starts from  $r=0$  and  $z=7$  cm (solid line), 8 cm (dashed line), 9 cm (dashed-dotted line) (b),  $r_p$  is normal to  $B$ -vector.  $B=50$  G,  $\alpha_B = 65^\circ$  and  $T_e=5$  eV.

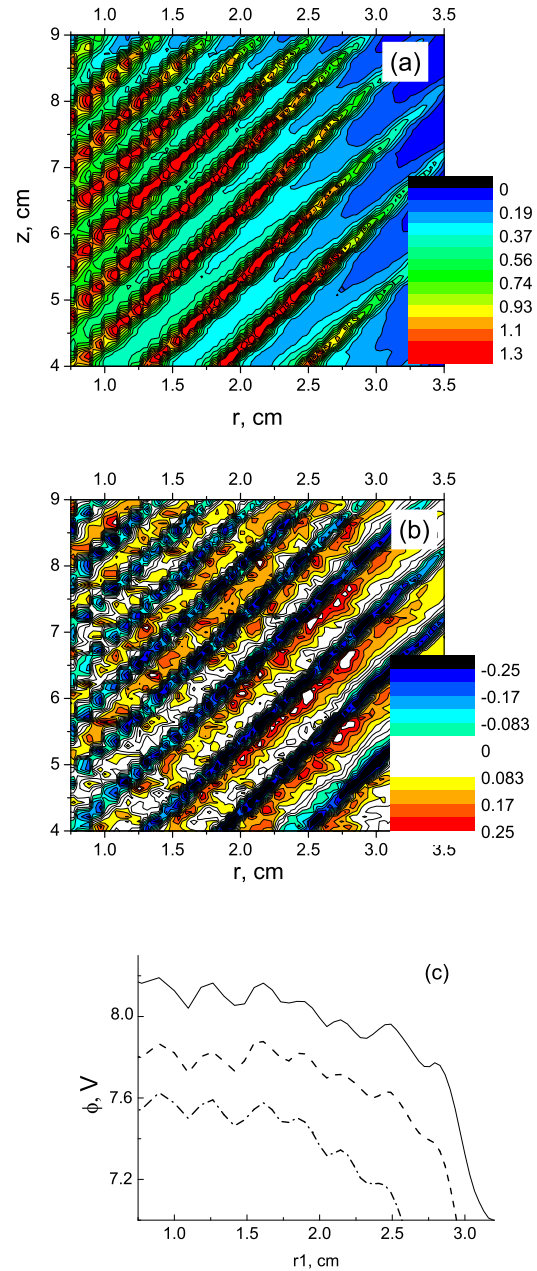


FIG. 5: Distributions of densities of electron  $n_e/10^8 \text{ cm}^{-3}$  (a) charge  $(n_e - n_i)/10^8 \text{ cm}^{-3}$  (b) and potential profile along axis  $r_p$  (normal to  $B$ -field) (c), which starts from  $r=0$ ,  $z=6$  cm (solid line), 6.5 cm (dashed line), 7 cm (dashed-dotted line), for  $B=100$  G,  $\alpha_B=65^\circ$  and  $T_e=10$  eV.

### EFFECT OF VARIATION OF ELECTRON TEMPERATURE AND B-FIELD

Fig.5(c) were taken across the  $B$ -field vector starting from  $r=0$  and  $z=6$  cm, 6.5 cm and 7 cm. The double-layers across  $B$ -vector have the potential drops of 0.2 V. For these cases we can distinguish seven double-layers.

As mentioned above the sheath with a small potential drop  $\delta\phi_w=3 \text{ eV} - 5 \text{ V}$  occurs over the grounded wall. The electrons with the energy larger than  $\delta\phi_w$  can overpass the sheath and escape from the plasma. Therefore the temperature of plasma electrons is smaller than  $T_e$



which sets the Maxwellian velocity distribution for electrons during ion-electron pair generation. In simulations, the mean electron energy  $\epsilon_e$  ranges from 1.6 eV to 3.4 eV for  $T_e=2.5$  eV - 10 eV for different strengths of B-field. An example of the plasma electron energy distribution for different  $T_e$  and B is shown in Fig.6. These energy profiles also reflect the specific structure of plasma in oblique magnetic confinement. As seen in Fig.6, for the same  $T_e=2.5$  eV the plasma electrons have essentially higher energy for B=100 G than for the case of B=25 G.

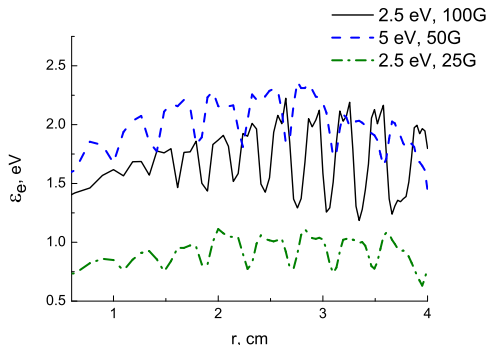


FIG. 6: Electron energy profile over radius for  $z=6$  cm,  $T_e=2.5$  eV,  $B=100$  G (solid line),  $T_e=5$  eV,  $B=50$  G (dashed line),  $T_e=2.5$  eV,  $B=25$  G (dotted-dashed line),  $\alpha_B=65^\circ$ .

In the limit of large  $r_L \sim T_e^{0.5}/B$  and small  $n_e$  the plasma becomes smoother since the Larmor radius and inter-peaks distance are comparable. With decreasing  $T_e^{0.5}/B$  and increasing  $n_e$  the plasma forms more and more sharp peaks. We resolve 19 peaks for the case of  $\alpha_B=65^\circ$  and  $r_L=0.07$  cm ( $T_e=2.5$  eV and  $B=100$  G).

Let us consider a modification of plasma characteristics with changing parameter  $r_L$  at given  $\alpha_B=65^\circ$ . The electron density profiles for two cases with close values of Larmor radii,  $r_L=0.075$  cm ( $T_e=2.5$  eV,  $B=50$  G) and  $r_L=0.05$  cm ( $T_e=5$  eV,  $B=100$  G) are shown in Fig.7(a). The broadenings of these density peaks are similar and equal approximately to  $2r_L$ . The  $n_e$ -profiles for two different values of  $r_L=0.15$  cm ( $T_e=2.5$  eV,  $B=25$  G) and  $r_L=0.038$  cm ( $T_e=2.5$  eV,  $B=100$  G) are shown in Fig.7(b). As expected the broadening of  $n_e$ -peaks is larger the former case with larger  $r_L$ .

In Fig.7(c), the  $n_e$ -profiles are shown for three values of  $r_L=0.075, 0.105, 0.15$  cm. For these variants we took  $B=50$  G and different  $T_e=2.5$  eV, 5 eV and 10 eV. A smoothed profile refers to the case with  $r_L=0.15$  cm and  $T_e=10$  eV. The  $n_e$ -profiles (3) Fig.7(c) and (1) in Fig.7(b) have very different shapes whereas  $r_L=0.15$  cm for both cases, but  $\lambda_D$  is larger for the former case.

With changing  $T_e$  from 5 eV to 2.5 eV, the size of quasineutral area increases since the wall potential drops from 5.1 eV to 3.6 eV. The number of ridges increases from 6 to 8 (see Fig.7(c)), but inter-peak gap diminishes as the  $\lambda_D$  decreases. It is seen that the characteristics

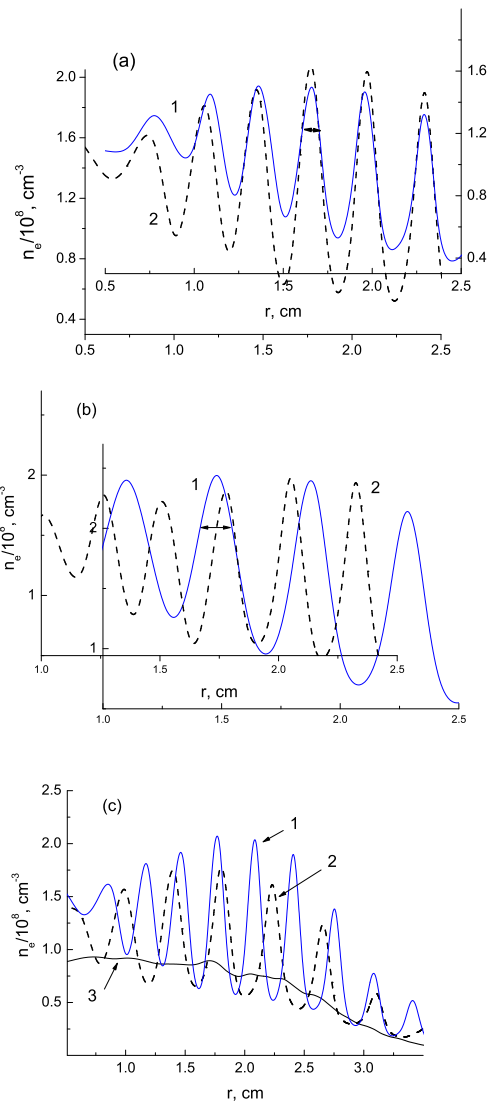


FIG. 7: Electron density profiles over radius at  $z=6$  cm (a) for  $r_L=0.075$  cm ( $T_e=2.5$  eV,  $B=50$  G) (1) and  $r_L=0.05$  cm ( $T_e=5$  eV,  $B=100$  G) (2), (b) for  $r_L=0.15$  cm ( $T_e=2.5$  eV and  $B=25$  G) (1) and  $r_L=0.038$  cm ( $T_e=2.5$  eV and  $B=100$  G) (2), (c) for  $B=50$  G and  $T_e=2.5$  eV ( $r_L=0.075$  cm) (1), 5 eV  $r_L=0.105$  cm (2) and 10 eV  $r_L=0.15$  cm (3).  $\alpha_B=65^\circ$ .

of structure reflect of an interplay of the wall potential drop,  $r_L$  and  $\lambda_D$ .

Period length of multi-steps double-layer structure is shown in Fig.8 as a function of  $r_L$  for  $\alpha_B=65^\circ$ . Note that  $\lambda_D$  slightly changes for different cases since the plasma density depends on the potential drop near the wall, which in turn is a function of the electron energy.

In conclusion, we have performed 2D3V PIC MCC simulations of dc discharge plasma in the cylindrical chamber at low gas pressure. The plasma is maintained by external ionization and confined by external oblique magnetic field. The periodical structure with ridges of ion and electron densities have been found for larger obliqueness

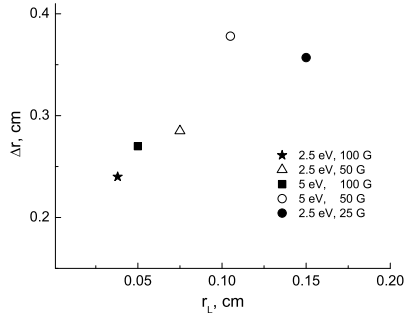


FIG. 8: Period length of periodical structure from  $r_L$  for different  $T_e$  and  $B$ ,  $\alpha_B = 65^\circ$ .

of magnetic field. The electron and ion ridges are shifted with respect to each other and double-layer structure appears across B-field and along the potential rise.

The double-layers form due to a distortion of local quasineutrality in the presence of oblique magnetic field. When electron-ion pair appears after an ionization event an electron begins Larmor gyromotion. The electron is shifted from the ion in the direction normal to B-field and a local charge appears.

The current flow channels are associated with ridges of electron and ion densities. They are aligned with  $B$ -vector not only in the area of quasineutral plasma, but also within the sheath over the wall. The modulation of electron current near the side wall in the plasma under similar conditions was registered in Ref.[10]. While our discharge geometry is not exactly the same we did not give the direct comparison of simulation and experimental results. However the phenomena of multiple layer formation observed in our simulations and in the experiment [10] in discharge plasma induced by the oblique magnetic field are very similar.

The ion current approaching side wall of the cylindrical chamber considerably increases and has a peaked profile in the case of large obliqueness of B-field. The ion current distribution over the cathode sheath demonstrates some focusing effect in magnetic field with larger angle  $\alpha_B$ .

The characteristics of plasma structure such as the

number of peaks, gap between them, their broadening depend on the Larmor radius ( $\sim T_e^{0.5}/B$ ), Debye length and the size of quasineutral plasma. The structure exists within some ranged of  $T_e^{0.5}/B$  and  $n_e$ . With increasing  $T_e^{0.5}/B$  and decreasing  $n_e$  the density peaks begin to overlap due to increasing broadening and the plasma loses the periodical structure.

The authors gratefully acknowledge FA9550-11-1-0160, Program Manager Mitat Birkan for support of this research. One of the authors, IVS, was partly supported by grant of Russian Foundation of Basic Research No. 15-02-02536.

- 
- [1] J. Miedzik, S. Barral and D. Danilko, Phys. Plasmas 22, 043511 (2015).
  - [2] K. G. Xu, H. Dao, and M. L. R. Walker, Phys. Plasmas 19, 103502 (2012).
  - [3] T. Intrator, J. Menard, and N. Hershkowitz, Physics of Fluids B, **5**, 806 (1993); doi: 10.1063/1.860933
  - [4] J. E. Borovsky and G. Joyce, J. Plasma Phys., **29**, 45 (1983).
  - [5] R. E. Ergun *et al.*, Phys.Rev.Lett. **87**(4), 045003 (2001).
  - [6] R. E. Ergun *et al.*, Phys. Rev. Lett., **102**(15), 155002 (2009).
  - [7] F. Mozer *et al.*, Phys. Rev. Lett., **111**(23), 235002 (2013).
  - [8] D. M. Malaspina *et al.*, Geophys. Res. Lett., **41** 5693 (2014); doi:10.1002/2014GL061109
  - [9] D. M. Malaspina *et al.*, J. Geophys. Res.: Space Phys. **120**, 4246 (2015).
  - [10] J. N. Lukas, Ph.D. thesis, George Washington University, 2016.
  - [11] K. Oksavik, C. van der Meeren, D. A. Lorentzen1, L. J. Baddeley, and J. Moen, J. Geophys. Res.: Space Phys. **120**, 9161 (2015).
  - [12] S. F. Gimelshein, V. A. Schweigert and M. S. Ivanov, in *Proc. of 21st Int. Symp. on Rarefied Gas Dynamics, Marseille, France, 1999*, edited by R. Brun et al. (Toulouse: Cepadues Editions, 1999), vol.2, p. 401; I. V. Schweigert, I. D. Kaganovich and V. I. Demidov, Phys. Plasmas, **20**, 101606 (2013); I. V. Schweigert, S. J. Langendorf, M. L. R. Walker and M. Keidar, Plasma Sources Sci. Technol., **24**, 025012 (2015).
  - [13] Ivanov V V, Popov A M and Rakhimova T V 1995 Sov. Plasma Phys. 21 548
  - [14] Lagushenko R and Maya J 1984 J. Appl. Phys. 59 3293